nature portfolio

https://doi.org/10.1038/s41586-025-09959-z

Supplementary information

Low-power integrated optical amplification through second-harmonic resonance

In the format provided by the
authors and unedited

I. SUPPLEMENTARY INFORMATION

A. SH-resonant OPA Derivations

We solve for the resonant second harmonic power in SH-resonant SHG by solving self-consistently for the power after one round trip pass. In the low-loss limit the SH is approximately constant throughout the SHG section

$$P_{\mathrm{SH}} \approx P_{\mathrm{SH}}(1-\gamma) + \eta_{\mathrm{SHG}} P_0 \tag{1}$$

where P_{SH} is the intracavity SH power just after the SHG section, γ is the round-trip loss (including any effective loss from OPA conversion), η_{SHG} is the SHG conversion efficiency, and P_0 is the input FH pump power. In contrast with linear resonators described by fields linearly interfering based on fixed coupling strengths, this nonlinear resonator is much simpler to describe in terms of power and conversion. Rearranging, we arrive at the equation in the text:

$$P_{\mathrm{SH}} = P_0 \frac{\eta_{\mathrm{SHG}}}{\gamma}, \qquad \text{where} \tag{2}$$

$$\eta_{\mathrm{SHG}} \approx 1 - e^{-2\sqrt{\eta_0 P_{\mathrm{SH}}}L}, \tag{3}$$

where the expression for η_{SHG} comes from integrating the nonlinear coupled-wave equations in the limit of constant SH power. This is a simple and powerful equation for describing SH-resonant OPA since it directly relates the measured SHG pump depletion to the expected phase-sensitive OPA gain by (for equal SHG and OPA nonlinear lengths) $\eta_{\mathrm{SHG}} = 1 - \frac{1}{G}$.

We also derive a more robust equation that is valid even for large round trip losses. Assuming about half the loss comes from the SHG section and using the exact solution for lossless SHG evolution,[1] we revise equation 2 to get

$$P_{\mathrm{SH,\,after}} = \left(1 - \frac{\gamma}{2}\right) \times P_{\mathrm{SH}}\left(L, \eta_0, P_0, \left(1-\frac{\gamma}{2}\right) P_{\mathrm{SH,\,after}}\right), \tag{4}$$

$$\eta_{\mathrm{SHG}} = \frac{P_0 - P_{\mathrm{FH}}(L, \eta_0, P_0, (1-\frac{\gamma}{2})P_{\mathrm{SH,\,after}})}{P_0} \tag{5}$$

where $P_{\mathrm{SH,\,after}}$ is the SH power just after the SHG section (an important clarification since the SH power is no longer near-constant throughout the resonator), $P_{\mathrm{SH}}(z, \eta_0, P_0, P_{\mathrm{SH,in}})$ and $P_{\mathrm{FH}}(z, \eta_0, P_0, P_{\mathrm{SH,in}})$ describes the lossless SH and FH evolution during the SHG section,[1] and $P_{\mathrm{SH,in}}$ is the SH power at the input to the SHG section.

We verify the validity of equations (2) and (4) by comparing them with full numerical simulations that directly solve the lossy nonlinear coupled wave equations for many round trips to find the steady-state SH power distribution. As shown in Figure 1d, the approximate model of equation 2 is valid up until fairly large losses ($\gamma \approx 0.5$) and the more precise model of equation 4 is robust for essentially all loss values. At very high losses, the solution approaches that of nonresonant SHG since the resonant enhancement disappears with loss.

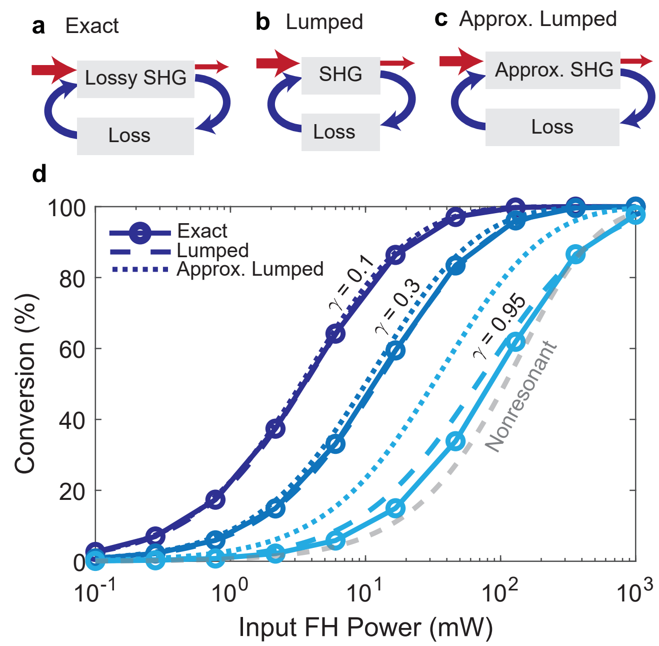

FIG. 1. **Validation of approximate model with numerics.** Numerical simulations and simple models for conversion efficiency of SH-resonant SHG, for various round-trip losses.

B. SH-resonant OPA Scaling with Length

The pump power in SH-resonant OPA depends on round-trip pump propagation losses

$$P_{\mathrm{SH}} \approx \frac{P_0 \eta_{\mathrm{SHG}}}{\gamma} = \frac{P_0 \eta_{\mathrm{SHG}}}{1 - e^{-2\alpha_{\mathrm{SH}} L_c}} \approx \frac{P_0 \eta_{\mathrm{SHG}}}{2\alpha_{\mathrm{SH}} L_c}, \tag{6}$$

where L_c represents the full cavity length and α_{SH} is the SH field propagation loss rate, and the last approximation was in the limit of small round trip losses. We can approximate $L_c \approx 2L$ if we assume most of the length of the cavity comes from the SHG and OPA nonlinear sections. Assuming sufficiently efficient SHG $\eta_{\mathrm{SHG}} \approx 1$, the length-dependence of the SH-resonant OPA equations becomes

$$G = e^{2\frac{g}{\sqrt{\gamma}}L} = e^{2g\frac{L}{\sqrt{2\alpha_{\mathrm{SH}} L_c}}} \approx e^{2g\sqrt{\frac{L}{4\alpha_{\mathrm{SH}}}}}. \tag{7}$$

The exponential scaling with square-root of nonlinear length suggests that long, low-finesse SH resonators are yield higher gains compared to short, high-finesse resonators with the same SH loss rate. As mentioned in the text, the maximum length is often fixed by bandwidth, fabrication variation, or footprint constraints. In quantum applications, required nonlinearity-to-loss ratio is another factor that could drive SH-resonant OPA designs towards smaller, higher-finesse resonators.

Note that the gain of nonresonant OPAs can also be limited by pump propagation losses. The OPA gains are modified in the presence of pump propagation losses by $L \to L_{\text{eff}}$, where the effective length captures the diminishing gain as the pump accrues losses:

$$L_{\text{eff}} = \frac{1 - e^{-\alpha_{\text{SH}} L}}{\alpha_{\text{SH}}}. \tag{8}$$

At small lengths, $L_{\text{eff}} \approx L$ and the effect of losses is negligible. At longer lengths, however, $L_{\text{eff}} \to \frac{1}{\alpha_{\text{SH}}}$ and the losses limit effective length and therefore gain.

C. Phase-sensitive Gain - Data Analysis

In this section we model the wavelength-dependent phase-sensitive amplification of the degenerate OPA measurements to arrive at the equation reported in the methods. The FH pump and degenerate seed beams are generated from a single input laser incident on a beamsplitter, travel different paths in fiber, and then are coupled onto the chip. The FH pump generates the SH pump, whose phase determines the amplification/deamplification quadratures for the seed light. The seed mixes with a small amount of FH pump leakage that is not entirely suppressed by the filters and then coupled into the OPA.

The phases of all the beams at the start of the OPA section depend on the effective path lengths L_i and propagation constants β_i:

$$\begin{aligned} \phi_{\text{seed}} &= \beta_{\text{FH}} L_{\text{seed}}, \\ \phi_{\text{SH}} &= 2(\beta_{\text{FH}} L_{\text{pump}}) + \beta_{\text{SH}} L_{\text{SHG}}, \\ \phi_{\text{leakage}} &= (\beta_{\text{FH}} L_{\text{pump}}) + \beta_{\text{FH}} L_{\text{SHG}}, \end{aligned}$$

where L_{SHG} is the small path length between the SHG and OPA sections and $L_{\text{seed}}, L_{\text{pump}}$ capture the large mostly-fiber path lengths traveled by seed and pump beams after the beamsplitter. Since the phase of the SH determines what quadratures are amplified and deamplified, we define the phases

$$\begin{aligned} \phi &\equiv \phi_{\text{SH}} - 2\phi_{\text{seed}} \qquad (9) \\ &= 2\beta_{\text{FH}}(L_{\text{pump}} - L_{\text{seed}}) + \beta_{\text{SH}} L_{\text{SHG}}, \\ \theta &\equiv \phi_{\text{SH}} - 2\phi_{\text{leakage}} \qquad (10) \\ &= (\beta_{\text{SH}} - 2\beta_{\text{FH}}) L_{\text{SHG}}. \end{aligned}$$

As we tune wavelength across a single SH resonance, the relative phase ϕ between SH and seed changes rapidly but the relative phase θ between SH and leakage is essentially constant due to the relatively small path length $L_{\text{SHG}} \ll L_{\text{pump}} - L_{\text{seed}}$.

The total seed input to the OPA is the linear interference between the injected seed and the (largely suppressed) FH pump leakage. With respect to the amplification and deamplification quadratures X_s and Y_s, the total seed quadratures are given by

$$\begin{aligned} X_s &= \sqrt{P_{s,0}} \cos\phi + \sqrt{P_l} \cos\theta, \\ Y_s &= \sqrt{P_{s,0}} \sin\phi + \sqrt{P_l} \sin\theta. \end{aligned}$$

The OPA amplifies one quadrature and deamplifies the other, resulting in output power

$$\begin{aligned} P &= G X_s^2 + \frac{1}{G} Y_s^2 \\ &= G\Big(P_{s,0}\cos^2\phi + P_l \cos^2\theta + 2\sqrt{P_{s,0}P_l}\cos\theta\cos\phi\Big) \\ &\quad + \frac{1}{G}\Big(P_{s,0}\sin^2\phi + P_l \sin^2\theta + 2\sqrt{P_{s,0}P_l}\sin\theta\sin\phi\Big) \\ &= P_{s,0}\left(G\cos^2\phi + \frac{1}{G}\sin^2\phi\right) \\ &\quad + P_l\left(G\cos^2\theta + \frac{1}{G}\sin^2\theta\right) \\ &\quad + 2\sqrt{P_{s,0}P_l}\left(G\cos\theta\cos\phi + \frac{1}{G}\sin\theta\sin\phi\right). \qquad (11) \end{aligned}$$

The first term is the desired OPA phase dependence that varies rapidly with wavelength, the second term is the amplified leakage that varies slowly with wavelength, and the last term is the undesired linear seed-leakage interference that varies rapidly with wavelength. In our measurements, the amplified leakage term was very small compared to the amplified signal (≈ 10 dB below). However, slight asymmetric oscillations due to the seed-leakage interference term could be observed for certain gains/seed powers, and also the limited bandwidth of the analog output channel of the optical spectrum analyzer partly smoothed over the most rapid oscillations with wavelength in equation. 11.

We extract the actual gain G from measured transmission G_{observed} by using a moving average filter with period equal to the oscillation period. The smoothing cancels out any linear interference terms and leaves just the desired average gain term incoherently added with the amplified leakage term:

$$\begin{aligned} \langle G_{\text{observed}} \rangle &= \frac{\langle P \rangle}{P_{s,0}} \\ &= \tfrac{1}{2}\left(G + \frac{1}{G}\right) \\ &\quad + \frac{P_l}{P_{s,0}}\left(G\cos^2\theta + \frac{1}{G}\sin^2\theta\right) \\ &= \tfrac{1}{2}\left(G + \frac{1}{G}\right) + \frac{P_{l,G}}{P_{s,0}}, \qquad (12) \end{aligned}$$

where we used the fact that the average over one oscillation of a sinusoid is equal to one half and defined $P_{l,G}$ to be the amplified leakage value for its near-constant phase θ. Solving for G:

$$G = \left(\langle G_{\text{observed}} \rangle - \frac{P_{l,G}}{P_{s,0}}\right) + \sqrt{\left(\langle G_{\text{observed}} \rangle - \frac{P_{l,G}}{P_{s,0}}\right)^2 - 1}$$

which in the high-gain and small-leakage limit simplifies to

$$G \approx 2\langle G_{\text{observed}}\rangle. \tag{13}$$

In practice, noise on observed gain can lead to negative terms inside the square root around unity gain. To make this equation robust, we restrict it to be real and arrive the equation reported in the methods.

D. Noise Figure Derivation

The on-chip noise figure of a phase-insensitive amplifier (PIA), assumed to be limited by signal-spontaneous beat noise and shot noise,[2] depends on the phase-insensitive net gain G_{net} and measured output spontaneous parametric fluorescence (SPF) level $\rho_{\text{ASE,out}}$:

$$NF_{\text{PIA}} = \frac{2\frac{\rho_{\text{ASE, out}}}{h\nu}}{G_{\text{net}}} + \frac{1}{G_{\text{net}}}$$

We can directly measure on-chip SPF level $\rho_{\text{ASE,out}}$ with the OSA (correcting for chip-OSA coupling efficiency). We extract net gain from measurements of on-off gain $G_{\text{on/off}}$, dichroic coupler input and output losses $1-\eta_1,\ \ 1-\eta_2$, and propagation losses $1-\eta_{\text{prop}}$

$$G_{\text{net}} = \eta_1\eta_2\eta_{\text{prop}}G_{\text{on/off}}.$$

The theoretical SPF level should account for the nonlinearity to loss ratio as discussed in,[3] but can be simply bounded by assuming half the propagation loss occurs before the amplifier and the other half after. The noise figure equation we use on our data and theory curves are therefore

$$\begin{aligned} NF_{\text{PIA, expt}} &= \frac{2\frac{\rho_{\text{ASE, out}}}{h\nu}}{\eta_1\eta_2\eta_{\text{prop}}G_{\text{on/off}}} \\ &\quad + \frac{1}{\eta_1\eta_2\eta_{\text{prop}}G_{\text{on/off}}} \qquad (14) \\ NF_{\text{PIA, theory}} &< \frac{2(\eta_2(\frac{1+\eta_{\text{prop}}}{2})G_{\text{on/off}}-1)}{\eta_1\eta_2\eta_{\text{prop}}G_{\text{on/off}}} \\ &\quad + \frac{1}{\eta_1\eta_2\eta_{\text{prop}}G_{\text{on/off}}} \qquad (15) \end{aligned}$$

Similarly, the phase-sensitive amplification noise figure is

$$\begin{aligned} NF_{\text{PSA}} &= \frac{\frac{G_{\text{PSA}}}{G_{\text{PIA}}}(\frac{\rho_{\text{ASE}}}{h\nu\Delta\nu}+1)}{G_{\text{PSA}}} \\ &= \left(\frac{\rho_{\text{ASE}}}{G_{\text{PIA}}h\nu} + \frac{1}{G_{\text{PIA}}}\right) \qquad (16) \end{aligned}$$

and our experimental and theoretical expressions are

$$\begin{aligned} NF_{\text{PSA, expt}} &= \frac{1}{\eta_1\eta_2\eta_{\text{prop}}}\frac{G_{\text{PSA,on/off}}}{G_{\text{PIA,on/off}}} \\ &\quad \times \left(\frac{\frac{\rho_{\text{ASE}}}{h\nu}}{G_{\text{PSA,on/off}}} + \frac{1}{G_{\text{PSA,on/off}}}\right) \qquad (17) \\ NF_{\text{PSA, theory}} &= \frac{\eta_2(\frac{1+\eta_{\text{prop}}}{2})(G_{\text{PIA,on/off}}-1)}{\eta_1\eta_2\eta_{\text{prop}}G_{\text{PIA,on/off}}} \\ &\quad + \frac{1}{\eta_1\eta_2\eta_{\text{prop}}G_{\text{PIA,on/off}}}, \qquad (18) \end{aligned}$$

where $G_{\text{PSA,on/off}}$ is the measured on-off gain and $G_{\text{PIA,on/off}}$ is the phase-insensitive on/off gain that corresponds to the measured phase-sensitive gain.

E. Saturation Effects

Saturation effects are out of the scope of this work and will be reported in a future study. Initial calculations reveal that the saturation behavior of SH-resonant OPA has some beneficial properties compared to nonresonant OPAs, since the SH power is stabilized and enhanced by the cavity. Furthermore, parasitic sum-frequency generation between the FH pump and signal, which contributes significantly to channel crosstalk in wavelength-division-multiplexed single-stage OPAs, does not occur in this design because the SHG and OPA sections are distinct and so the FH pump and signal do not overlap.[4]

[1] Li, R.-D. & Kumar, P. Evolution of quantum noise in the traveling-wave second-order $\chi(2)$ nonlinear process. *J. Opt. Soc. Am. B* **12**, 2310–2320 (1995).
[2] Baney, D. M., Gallion, P. & Tucker, R. S. Theory and measurement techniques for the noise figure of optical amplifiers. *Optical Fiber Technology* **6**, 122–154 (2000).
[3] Ye, Z. *et al.* Overcoming the quantum limit of optical amplification in monolithic waveguides. *Science Advances* **7**, eabi8150 (2021).
[4] Li, X. *et al.* Two-stage lithium niobate nonlinear photonic circuits for low-crosstalk and broadband all optical wavelength conversion. *APL Photonics* **10**, 076121 (2025).